

# Copper ATPase CopA from *Escherichia coli*: Quantitative Correlation between ATPase Activity and Vectorial Copper Transport

Chathuri J. K. Wijekoon,<sup>†,§</sup> Saumya R. Udagedara,<sup>†,§,¶</sup> Roland L. Knorr,<sup>‡</sup> Rumiana Dimova,<sup>‡</sup> Anthony G. Wedd,<sup>\*,†</sup> and Zhiguang Xiao<sup>\*,†,¶,Ⓜ</sup>

<sup>†</sup>School of Chemistry and Bio21 Molecular Science and Biotechnology Institute, University of Melbourne, Parkville, Victoria 3010, Australia

<sup>¶</sup>The Florey Institute of Neuroscience and Mental Health, University of Melbourne, Parkville, Victoria 3010, Australia

<sup>‡</sup>Max Planck Institute of Colloids and Interfaces, Science Park Golm, 14424 Potsdam, Germany

**S** Supporting Information

**ABSTRACT:** Cu-ATPases are membrane copper transporters present in all kingdoms of life. They play a central role in Cu homeostasis by pumping Cu ions across cell membranes with energy derived from ATP hydrolysis. In this work, the Cu-ATPase CopA from *Escherichia coli* was expressed and purified in fully functional form and demonstrated to bind Cu(I) with subfemtomolar affinity. It was incorporated into the lipid membrane of giant unilamellar vesicles (GUVs) whose dimensions match those of eukaryotic cells. An <sup>1</sup>H NMR approach provided a quantitative ATPase activity assay for the enzyme either dissolved in detergent or embedded in GUV membranes. The activity varied with the Cu(I) availability in an optimized assay solution for either environment, demonstrating a direct correlation between ATPase activity and Cu(I) transport. Quantitative analysis of the Cu content trapped by the GUVs is consistent with a Cu:ATP turnover ratio of 1.

Cu-ATPases are selective for Cu(I) and are essential for activation of copper-dependent enzymes and for removal of excess copper from cells.<sup>1–4</sup> Inactivation of the human Cu pumps ATP7A/7B is associated with the copper imbalance characteristic of Menkes and Wilson diseases and of a spectrum of neuropathologies.<sup>5,6</sup>

In the past decade, extensive in cellulo studies have advanced our understanding of the cellular functions of Cu-ATPases.<sup>3</sup> Pathfinding achievements by Solioz, Rosen, and Argüello have underpinned the progress on the biochemistry of bacterial Cu-ATPases (named CopA).<sup>4,7–10</sup> However, the molecular mechanisms of binding and transport of Cu(I) across closed membrane vesicles and their coupling to ATP hydrolysis remain speculative. This report details a quantitative approach that demonstrates a correlation between ATPase activity and vectorial Cu transport for the CopA from *Escherichia coli* (EcCopA).

Cu-ATPases display a conserved topology (Figure 1a). Structures of CopA from *Legionella pneumophila* (78.2 kDa; LpCopA; 2.8–3.2 Å resolution) have been solved for two Cu-free forms and are the sole structures available for this class of P<sub>1B</sub>-type ATPases.<sup>11,12</sup> EcCopA and LpCopA possess 38%

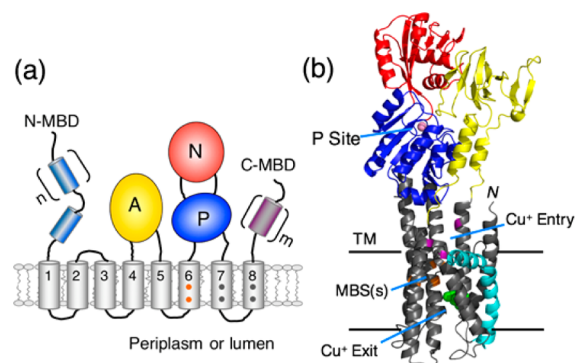


**Figure 1.** (a) Conserved topology of Cu-ATPases. (b) Model structure of EcCopA obtained using the determined structure of LpCopA (PDB entry 3RFU) as a template. Proposed sites for phosphorylation (pink), Cu<sup>+</sup> entry (purple), binding (orange), and exit (green) are indicated.

identity and 73% similarity for their overlapping sequences of 737 residues, and a model of EcCopA can be generated using the LpCopA structure as a template (Figure 1b). EcCopA features two N-terminal metal binding domains (N-MBDs), each of which possesses a Cys-xx-Cys binding site for Cu(I). The single N-MBD in LpCopA was not resolved in the structures.<sup>11</sup>

The color coding of Figure 1 connects the topology to the structure. In particular, the TM2 helix is kinked at a conserved double glycine site, forming a positively charged “landing platform” (in cyan) for a potential negatively charged Cu(I)-donating carrier (but see ref 13 for special cases).<sup>11,14</sup> The N, P, and A domains connect the energy of ATP hydrolysis to the pumping of Cu(I) across the membrane. Potential metal binding ligands are present in TM6–8, including the fingerprint CPC motif in TM6 (see dots in Figure 1a).

EcCopA (87.9 kDa) was expressed initially as a fusion protein with a His-tagged C-terminal green fluorescent protein (GFP) (see the Supporting Information (SI)).<sup>15</sup> Confocal microscopy on transformed *E. coli* cells expressing EcCopA-GFP confirmed insertion of the target into its native inner membrane (Figure 2a). The intact fusion protein, upon

**Received:** December 15, 2016

**Published:** March 8, 2017

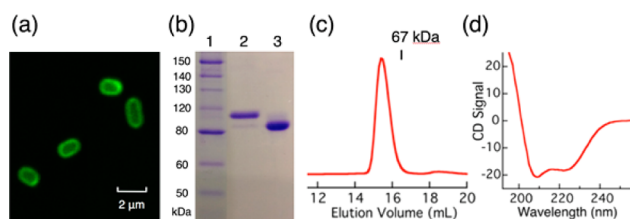


**Figure 2.** (a) Confocal microscopy of *E. coli* cells expressing EcCopA-GFP to the cell inner membrane. (b) SDS-PAGE of purified protein samples: (1) markers; (2) EcCopA-GFP; (3) EcCopA. (c) Elution profile of EcCopA from a Superdex 200 gel-filtration column (the elution position of a standard albumin (67 kDa) is marked). (d) Far-UV CD spectrum of EcCopA in KPi buffer (pH 7.4, 0.01% DDM).

solubilization in the detergent *n*-dodecyl  $\beta$ -D-maltoside (DDM; critical micelle concentration = 170  $\mu$ M), was purified with a nickel-based affinity column followed by gel filtration (Figure 2b, lane 2; SI 3). Expression of the EcCopA gene alone provided GFP-free samples at 4–6 mg per liter of cell culture (Figure 2b, lane 3; SI 3).

Purified EcCopA was intact structurally: (i) it eluted from a gel-filtration column as a symmetric peak at a position consistent with the expected molar mass (Figure 2c); (ii) the circular dichroism (CD) spectrum indicated high  $\alpha$ -helix content (Figure 2d; cf. Figure 1); and (iii) the protein concentrations estimated via absorbance at 280 nm based on the primary sequence matched those estimated via thiol assays of the fully reduced samples, as the 4 equiv of cysteinyl thiols present in the two N-MBDs were detected in the detergent DDM along with a further 2 equiv from the CPC motif in TM6 upon unfolding of the protein with the denaturing detergent SDS (SI 5, Figure S1, and Table S2).

EcCopA exhibits high affinity for Cu(I) (SI 6). Titration into a solution of  $[\text{Cu}^{\text{I}}(\text{Bca})_2]^{3-}$  ( $\log \beta_2 = 17.3$ )<sup>16</sup> led to quantitative transfer of 2 equiv of Cu(I) from the probe complex to the enzyme (Figure S2), while an equivalent titration employing  $[\text{Cu}^{\text{I}}(\text{Bcs})_2]^{3-}$  ( $\log \beta_2 = 19.9$ )<sup>16</sup> as the probe revealed an effective competition and an estimated apparent average affinity of  $\log K_{\text{D}} = -17.6$  at pH 7.4 (Figure S3). The two isolated individual N-MBDs were shown to bind 1 equiv of Cu(I) each with similar affinities,<sup>17</sup> but the nature of Cu(I) binding detected for the intact EcCopA under the present conditions remains to be explored.

ATPase activity was evaluated by <sup>1</sup>H NMR detection of both the reactant, ATP, and the product, ADP.<sup>18</sup> The advantages relative to detection of product inorganic phosphate (Pi)<sup>19,20</sup> or ion exchange chromatography<sup>21</sup> include (i) continuous monitoring of ATP hydrolysis, (ii) small sample size, and (iii) toleration of complex sample conditions, including the presence of detergents, lipids, phosphate, and Cu(I) complexes. The assay detects the resolved <sup>1</sup>H NMR signals of the purine H8 protons of ATP and ADP (Figure 3a).<sup>18</sup> The experiments were conducted at 37 °C in an optimized assay solution containing DDM (see Table 1, Figure S4, and SI 7). ATP was stable in this solution in the presence or absence of Cu(I) but was hydrolyzed catalytically upon addition of EcCopA (0.5–1.5  $\mu$ M) under a range of conditions (Figure 3b and Table 1). The hydrolysis rate increased proportionally with the enzyme concentration, allowing reliable estimation of the ATPase activity under each set of conditions (Figure 3c and Table 1).

Active enzyme must be in its reduced form<sup>22</sup> and was inhibited completely by vanadate (0.2 mM), which binds

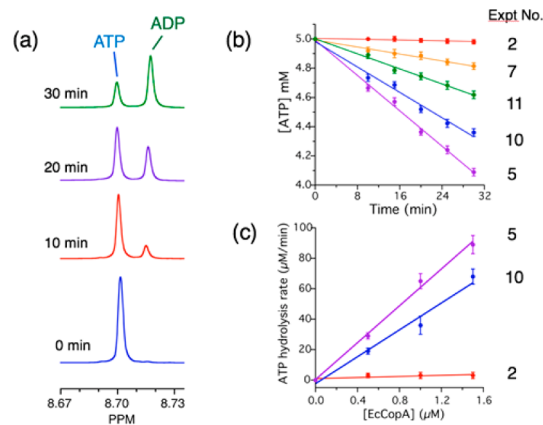


**Figure 3.** Catalysis in DDM solution. (a) <sup>1</sup>H NMR detection of ATP hydrolysis catalyzed by EcCopA (1.5  $\mu$ M) in the presence of Bca (0.1 mM). (b) Catalytic time course for selected experiments of Table 1 at  $[\text{EcCopA}] = 0.5 \mu\text{M}$ . (c) Linear correlation of reaction rate vs  $[\text{EcCopA}]$  for experiments 2, 5, and 10.

irreversibly to the P-domain phosphorylation site (Table 1, experiment 2 and Figures 1 and 3b,c).

The ATPase activity was promoted by Cu(I), but a low level of background activity persisted despite a vigorous restriction of Cu availability (experiment 3). A maximal increase in the activity by  $60 \pm 4 \text{ min}^{-1}$  was achieved by added Cu that was stabilized by either GSH (as polymeric Cu(I)–GSH complexes)<sup>23</sup> or Bca (as  $[\text{Cu}^{\text{I}}(\text{Bca})_2]^{3-}$ ) and was insensitive to the concentration of either ligand (experiments 4 and 5; Figure S4a,b). Both systems buffer free  $[\text{Cu}^{\text{I}}]$  within the pico- to femtomolar range (Table 1 and Figure S5)<sup>16</sup> and cannot compete effectively with EcCopA for Cu(I) (see Figure S2). This maximal activity is a factor of 4–25 higher than those estimated previously for this enzyme ( $27\text{--}130 \text{ nmol mg}^{-1} \text{ min}^{-1}$ , i.e.,  $2.4\text{--}11.4 \text{ min}^{-1}$ ).<sup>8,17,24</sup> The present study had the advantage of more quantitative approaches and optimized conditions.

When free  $[\text{Cu}^{\text{I}}]$  was buffered by the ligand Bcs to the subfemtomolar range, the ATPase activity dropped and became sensitive to the ligand concentration (experiments 6–8). This is consistent with effective competition for Cu(I) between the Bcs ligand and EcCopA protein (Figure S3).

However, the Cu(I) complex of the isolated individual N-MBD6 of ATP7B is a robust Cu(I) donor for EcCopA despite its attomolar affinity for Cu(I).<sup>25</sup> Significantly, excess apo-MBD6 limits free  $[\text{Cu}^{\text{I}}]$  to  $10^{-18} \text{ M}$  but does not hinder promotion of the ATPase activity by its Cu(I) complex (experiments 9 and 10). It appears that direct protein–protein interactions between negatively charged  $\text{Cu}^{\text{I}}$ –MBD6 and the positively charged TM2 “landing platform” of EcCopA expedite Cu(I) transfer.<sup>26,27</sup> In support, the positively charged human copper chaperone  $\text{Cu}^{\text{I}}$ –Atox1 was less efficient in activating the ATPase activity, despite comparable Cu(I) binding affinity (Figure 3b; experiment 11 vs experiments 9 and 10).

Taken together, the above experiments demonstrate that (i) Cu(I) stimulates EcCopA ATPase activity<sup>8,17</sup> and (ii) EcCopA competes for Cu(I) with subfemtomolar affinity.<sup>17</sup> These properties are consistent with its role in removing excess Cu(I) from the bacterial cytosol.<sup>1</sup>

The requirement of Cu(I) for optimal ATPase activity supports the suggestion that this activity is coupled to enzyme-mediated Cu(I) translocation.<sup>10</sup> However, this speculation

Table 1. ATPase Activity of EcCopA Dissolved in DDM Solution and Embedded in GUVs and Correlated Cu Uptake by GUVs

expt no.	Cu(I) ligand L	DDM (0.01% w/v) <sup>a</sup>				EcCopA-GUVs <sup>a</sup>					
		[L] <sub>tot</sub> (μM)	[Cu] <sub>tot</sub> (μM)	pCu <sup>+</sup> <sup>b</sup>	ATPase activity (min <sup>-1</sup> ) <sup>c,d</sup>	[L] <sub>tot</sub> (mM)	[Cu] <sub>tot</sub> (μM)	pCu <sup>+</sup> <sup>b</sup>	ATPase activity (min <sup>-1</sup> ) <sup>c,d</sup>	Cu(I) uptake (min <sup>-1</sup> ) <sup>d</sup>	Cu/ATP
1 <sup>e</sup>	GSH <sup>f</sup>					1.0	300	<15	—	0	—
2 <sup>g</sup>	GSH <sup>f</sup>	100	10	~15	<1	1.0	300	<15	0	0	—
3	Bcs	100–500	<1	—	12(1)	0.5–1.5	~1	—	6.0(5)	<0.5	<0.1
4	GSH	50–500	10	~15	60(3)	0.7–1.2	300	<15	26(2)	23(1)	0.9
5	Bca	25–250	10	12–15	58(2)	0.7–1.2	300	<15	27(3)	24(2)	0.9
6	Bcs	25	10	14.3	47(3)	0.75	300	15.8	21(2)	18(1)	0.9
7	Bcs	100	10	16.7	12(1)	1.0	100	17.7	6.0(5)	—	—
8	Bcs	400	10	18.1	10(1)	1.2	100	17.9	4.0(5)	3.3(5)	0.8
9	MBD6	11	10	16.9	43(2)	0.35	300	17.1	17(1)	14(1)	0.8
10	MBD6	30	10	18.1	44(2)	0.9	300	18.2	17(1)	—	—
11	Atox1	11	10	16.8	25(2)	0.35	300	18.1	14(1)	12(1)	0.9

<sup>a</sup>Other components: ATP (5.0 mM), MgCl<sub>2</sub> (5.0 mM), NaCl (50 mM), D<sub>2</sub>O (40% v/v), GSH (0.1 mM), ascorbate (0.5 mM), Na-Mops buffer (50 mM, pH 7.4), plus Cu and ligands L as indicated. <sup>b</sup>Values of free pCu<sup>+</sup> (= -log [Cu<sup>+</sup>]) buffered by the polymeric Cu(I)–GSH complexes<sup>23</sup> were estimated approximately from Figure S5 and those by other complexes were calculated using the relevant constants at pH 7.4: log β<sub>2</sub> = 17.3 for [Cu<sup>I</sup>(Bca)<sub>2</sub>]<sup>3-</sup> and 19.9 for [Cu<sup>I</sup>(Bcs)<sub>2</sub>]<sup>3-</sup>; <sup>16</sup> log K<sub>D</sub> = -17.8 for Cu<sup>I</sup>–Atox1<sup>16</sup> and -17.9 for Cu<sup>I</sup>–MBD6.<sup>25</sup> <sup>c</sup>Conducted at 37 °C; persistent residual activity was detected in controls that contained Bcs (0.1–1.5 mM) but no added Cu (see experiment 3) and was subtracted as background from the activities stimulated by the added Cu. <sup>d</sup>The value in each set of parentheses refers to error in the last digit averaged over three to five independent measurements. <sup>e</sup>ATP absent. <sup>f</sup>Added Bca gave an equivalent result. <sup>g</sup>EcCopA was either absent or premixed with [HVO<sub>4</sub>]<sup>2-</sup> (0.2 mM).

cannot be tested by the above experimental settings, and enclosed membrane vesicles must be employed. Giant unilamellar vesicles (GUVs) have been proposed as viable biomimetic cells with diameters typical of eukaryotic cells (10–100 μm).<sup>28</sup> GUVs (10–60 μm in diameter) prepared by electroformation from the lipid 1-palmitoyl-2-oleoyl-*sn*-glycero-3-phosphocholine (POPC) under appropriate conditions were compatible with the EcCopA system (SI 8–10). Enzyme incorporation was achieved by incubation with DDM-solubilized EcCopA followed by DDM removal with Biobeads (Figure 4 and SI 9).

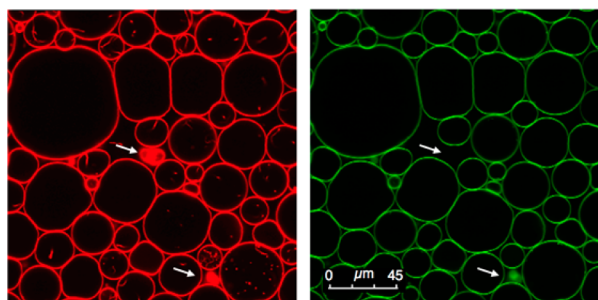


Figure 4. Confocal image of EcCopA-GFP GUVs with excitation at 594 nm for the lipid POPC-Texas Red (0.05% w/w) membrane (left) and at 488 nm for the CopA-GFP label (right). Red spots, including the two identified with arrows, are aggregates that incorporated little CopA protein. The GUVs are robust and separate upon dilution for analysis (see SI 10 and Figure S6).

Steady-state ATPase activity was detected for EcCopA GUVs following the same experimental protocol for EcCopA in DDM but with increased concentrations of each Cu(I) complex (Table 1). The observed activities followed the same order as those for EcCopA in homogeneous DDM solution but were reduced by 50–60%. This may be due to (i) access to EcCopA being constrained by local suspension in GUVs, (ii) loss of EcCopA-GUVs in the preparation (see SI 10c), and/or (iii) embedded EcCopA not being inserted uniformly in a single orientation poised for Cu transport (Figure 5a).

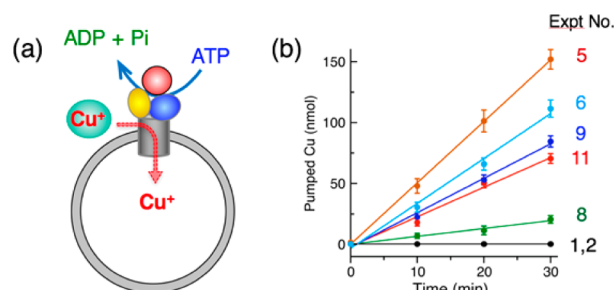


Figure 5. ATP-dependent vectorial copper transport: (a) experimental model; (b) analysis of Cu uptake by GUVs for selected examples from Table 1 (see SI 10 for details).

The observed ATPase activity of EcCopA in GUVs was confirmed to be coupled with active pumping of Cu<sup>+</sup> into the GUVs (Figure 5b; Tables 1 and S3; SI 10). Controls in the absence of ATP or with EcCopA being disabled by [HVO<sub>4</sub>]<sup>2-</sup> exhibited no Cu uptake by GUVs (Figure 5b and Table 1, experiments 1 and 2), demonstrating the absence of Cu leakage or passive diffusion and that the observed Cu uptake relied completely on active transportation. Neither Mg<sup>2+</sup> nor ATP were trapped in the experiments, despite the presence of high levels of both (5.0 mM) in the external solutions (SI 10a).

Significantly, the level of Cu trapped by the GUVs was correlated with the observed ATPase activities in a relationship of  $0.9 \pm 0.1$  Cu ions translocated per ATP hydrolysis, independent of the Cu(I) carrier (Table 1 and SI 10). The external free [Cu<sup>+</sup>] concentrations were buffered by the various Cu(I) ligands to at least subpicomolar levels (Table 1), but exclusion of such Cu(I) ligands from the internal solution had little impact on the Cu uptake experiments (SI 8), further demonstrating active Cu transport.

This is the first quantitative correlation of ATPase activity and Cu translocation for a P<sub>1B</sub>-type ATPase. The finding that one Cu(I) is pumped per ATP hydrolysis contrasts with the observation that two Ca<sup>2+</sup> ions are pumped in the Ca-ATPases,<sup>29</sup> upon which the current model of the Cu-ATPases is based.<sup>4,12</sup> However, it must be remembered that the copper

pumps evolved before the calcium pumps and that the chemistry of their metal ion pumping differs dramatically.<sup>3</sup>

## ■ ASSOCIATED CONTENT

### ● Supporting Information

The Supporting Information is available free of charge on the ACS Publications website at DOI: 10.1021/jacs.6b12921.

Experimental procedures, results, and discussion, Tables S1–S3, and Figures S1–S6 (PDF)

## ■ AUTHOR INFORMATION

### Corresponding Authors

\*z.xiao@florey.edu.au

\*agw@unimelb.edu.au

### ORCID

Zhiguang Xiao: 0000-0001-6908-8897

### Present Address

<sup>¶</sup>Current address: Department of Biochemistry and Genetics, La Trobe University, Melbourne, Victoria 3086, Australia.

### Author Contributions

<sup>§</sup>C.J.K.W. and S.R.U. contributed equally.

### Notes

The authors declare no competing financial interest.

## ■ ACKNOWLEDGMENTS

This work was supported by the Australian Research Council (Grant DP130100728) and is part of the MaxSynBio consortium, which is jointly funded by the Federal Ministry of Education and Research of Germany and the Max Planck Society. Some of the confocal images were recorded at the microscopy platform of the Bio21 Institute. Professor Svetlana Lutsenko (Johns Hopkins University) and Professor Ashley Bush (the Florey Institute) are thanked for comments and discussions.

## ■ REFERENCES

- (1) Rensing, C.; Grass, G. *FEMS Microbiol. Rev.* **2003**, *27*, 197–213.
- (2) Palmgren, M. G.; Nissen, P. *Annu. Rev. Biophys.* **2011**, *40*, 243–66.
- (3) Gupta, A.; Lutsenko, S. *Curr. Genomics* **2012**, *13*, 124–33.
- (4) Rosenzweig, A. C.; Argüello, J. M. *Curr. Top. Membr.* **2012**, *69*, 113–36.
- (5) Barnham, K. J.; Bush, A. I. *Curr. Opin. Chem. Biol.* **2008**, *12*, 222–8.
- (6) Collins, J. F.; Prohaska, J. R.; Knutson, M. D. *Nutr. Rev.* **2010**, *68*, 133–147.
- (7) Solioz, M.; Vulpe, C. *Trends Biochem. Sci.* **1996**, *21*, 237–241.
- (8) Fan, B.; Rosen, B. P. *J. Biol. Chem.* **2002**, *277*, 46987–92.
- (9) Sitsel, O.; Grønberg, C.; Autzen, H. E.; Wang, K.; Meloni, G.; Nissen, P.; Gourdon, P. *Biochemistry* **2015**, *54*, 5673–5683.
- (10) Argüello, J. M.; Patel, S. J.; Quintana, J. *Metallomics* **2016**, *8*, 906–14.
- (11) Gourdon, P.; Liu, X. Y.; Skjorringe, T.; Morth, J. P.; Møller, L. B.; Pedersen, B. P.; Nissen, P. *Nature* **2011**, *475*, 59–64.
- (12) Andersson, M.; Mattle, D.; Sitsel, O.; Klymchuk, T.; Nielsen, A. M.; Møller, L. B.; White, S. H.; Nissen, P.; Gourdon, P. *Nat. Struct. Mol. Biol.* **2014**, *21*, 43–48.
- (13) Fu, Y.; Bruce, K. E.; Wu, H.; Giedroc, D. P. *Metallomics* **2016**, *8*, 61–70.
- (14) Gonzalez-Guerrero, M.; Argüello, J. M. *Proc. Natl. Acad. Sci. U. S. A.* **2008**, *105*, 5992–5997.
- (15) Hsieh, J. M.; Besserer, G. M.; Madej, M. G.; Bui, H.-Q.; Kwon, S.; Abramson, J. *Protein Sci.* **2010**, *19*, 868–880.

- (16) Xiao, Z.; Brose, J.; Schimo, S.; Ackland, S. M.; La Fontaine, S.; Wedd, A. G. *J. Biol. Chem.* **2011**, *286*, 11047–11055.
- (17) Drees, S. L.; Beyer, D. F.; Lenders-Lomscher, C.; Lübben, M. *Mol. Microbiol.* **2015**, *97*, 423–438.
- (18) Guo, B.; Gurel, P. S.; Shu, R.; Higgs, H. N.; Pellegrini, M.; Mierke, D. F. *Chem. Commun.* **2014**, *50*, 12037–12039.
- (19) Lanzetta, P. A.; Alvarez, L. J.; Reinach, P. S.; Candia, O. A. *Anal. Biochem.* **1979**, *100*, 95–97.
- (20) Geladopoulos, T. P.; Sotiroudis, T. G.; Evangelopoulos, A. E. *Anal. Biochem.* **1991**, *192*, 112–116.
- (21) Bartolini, M.; Wainer, I. W.; Bertucci, C.; Andrisano, V. *J. Pharm. Biomed. Anal.* **2013**, *73*, 77–81.
- (22) The EcCopA enzyme isolated under oxidizing conditions was inactive but could be reactivated upon incubation with GSH (500  $\mu$ M) together with a catalytic amount of human glutaredoxin 1 enzyme (0.1  $\mu$ M) for 1–2 h. The latter acts as a catalyst for reduction of protein disulfides by GSH. See: Brose, J.; La Fontaine, S.; Wedd, A. G.; Xiao, Z. *Metallomics* **2014**, *6*, 793–808.
- (23) Corazza, A.; Harvey, I.; Sadler, P. J. *Eur. J. Biochem.* **1996**, *236*, 697–705.
- (24) Padilla-Benavides, T.; George Thompson, A. M.; McEvoy, M. M.; Argüello, J. M. *J. Biol. Chem.* **2014**, *289*, 20492–20501.
- (25) Wijekoon, C. J. K.; Ukuwela, A. A.; Wedd, A. G.; Xiao, Z. *J. Inorg. Biochem.* **2016**, *162*, 286–294.
- (26) Banci, L.; Bertini, I.; Calderone, V.; Della-Malva, N.; Felli, I. C.; Neri, S.; Pavelkova, A.; Rosato, A. *Biochem. J.* **2009**, *422*, 37–42.
- (27) Achila, D.; Banci, L.; Bertini, I.; Bunce, J.; Ciofi-Baffoni, S.; Huffman, D. L. *Proc. Natl. Acad. Sci. U. S. A.* **2006**, *103*, 5729.
- (28) Dezi, M.; Di Cicco, A.; Bassereau, P.; Levy, D. *Proc. Natl. Acad. Sci. U. S. A.* **2013**, *110*, 7276–81.
- (29) Inesi, G.; Tadini-Buoninsegni, F. *J. Cell Commun. Signal.* **2014**, *8*, 5–11.